Mechanisms and Impacts of a Partial AMOC Recovery Under Enhanced Freshwater Forcing

M. D. Thomas[1], A. V. Fedorov[1]

[1]Department of Geology and Geophysics, Yale University, New Haven, 06511

Key Points:

- We isolate a feedback mechanism for a partial AMOC recovery following a simulated AMOC weakening
- The heat transported by the weakening AMOC becomes more efficient as its upper branch warms
- Similar results from a 2D model demonstrate the recovery arises through an ocean-only 2D mechanism

Corresponding author: M. D. Thomas, `matthew.thomas@yale.edu`

Abstract

The Atlantic Meridional Overturning Circulation (AMOC) is expected to weaken in the 21st century due to increased surface buoyancy. Such AMOC changes in ocean models are often accompanied by a subsurface reduction in density. Here we perform freshwater perturbation experiments with both a 1° coupled model and an idealized zonally averaged ocean-only model to demonstrate that slow subsurface property changes (1) introduce a negative feedback that erodes the stratification and partially reinvigorates convection and the AMOC, and (2) ensure the meridional heat transport weakens less than the AMOC. In the coupled model with a 0.1 Sv net freshwater flux introduced around Greenland, an initial 22% AMOC reduction over 40 years is followed by a recovery of almost half the lost strength after 400 years. The final heat transport, however, is weakened by only 7%. Similar responses in the idealized model demonstrate that 2D ocean-only dynamics control the changes.

1 Introduction

Climate predictions using numerical and theoretical models of the ocean circulation almost universally agree that the Atlantic Meridional Overturning Circulation (AMOC) will weaken over the coming century under global warming. Projections of increased future rates of glacial runoff (IPCC, 2013), rainfall (Held and Soden, 2006), and surface heating (Cheng et al., 2017; Levitus et al., 2000) near high latitude regions of deep water formation imply the ocean there will become increasingly stratified, thereby inhibiting the convection that precedes overturning (Eden and Willebrand, 2001; Sevellec et al., 2017; Spall and Pickart, 2001; Thomas et al., 2015). The climatic consequences of a weakening AMOC on its transports of heat, freshwater and carbon (e.g. Rhines et al., 2008), which have played key roles in bringing about past climatic events (e.g. Menviel et al., 2014; Rahmstorf, 2002), have motivated the deployment of international observing arrays that provide continuous measurements of its strength in the Atlantic Ocean, including the RAPID array (Kanzow et al., 2007) and the recent Observing the Subpolar North Atlantic Program (OSNAP) array (Lozier et al., 2017). How we interpret the future impacts of any observed and predicted AMOC trends is therefore of great importance. However, a commonly overlooked possibility is the potential for the AMOC to recover part or all of its strength following an initial climate-change induced weakening (Manabe and Stouffer, 1994). We revisit this possibility here, isolating a North Atlantic ocean feed-

back mechanism for a partial AMOC recovery and, crucially, an even stronger recovery in its heat transport.

The question of whether the AMOC can recover following a climate change-induced collapse has been addressed in a number of previous 'hosing' experiments using climate models, in which a large amount of freshwater is artificially fluxed into the North Atlantic over a finite period of time (e.g. Brunnabend and Dijkstra, 2017; den Toom et al., 2014; Jackson and Vellinga, 2013; Liu et al., 2017; Mignot et al., 2007; Vellinga and Wood, 2008; Wood et al., 2003; Zhang and Delworth, 2005). Here, however, we instead address how the AMOC will respond on multi-decadal timescales to a high latitude freshwater flux that is both modest enough to retain an active AMOC and sustained continuously in time. Common interpretations of observed and modeled AMOC weakening trends are that it will monotonically weaken towards either a collapsed state or a new weaker steady state. However, a number of studies using models (e.g. Barreiro et al., 2008; Fedorov et al., 2007; Liu et al., 2009; Marcott et al., 2011; Mignot et al., 2007; Sevellec and Fedorov, 2015; Zhang et al., 2017) and paleo temperature reconstructions (Rasmussen and Thomsen, 2004; Ruhlemann et al., 2004) have now demonstrated that a weakening of the AMOC is accompanied by a gradual warming of the subsurface ocean. This therefore raises the possibility that the initial stratification introduced by a surface freshwater influx could be slowly eroded by subsurface changes in density, so that convection and the AMOC could be re-invigorated. This would follow a two-timescale response to both the initial stratification and the mechanism of the downwards transfer of buoyancy.

The possibility of an AMOC recovery under sustained but moderate climate change forcing was demonstrated by Manabe and Stouffer (1994) using a coupled ocean-atmosphere model with a 1% yr^{-1} CO_2 increase maintained for 70 years before being held constant. After an initial AMOC weakening in the model, by over a factor of 2 over the first 150 years, it then fully recovered by year 500. A similar AMOC recovery after an initial weakening was recently reported from an idealized configuration of an ocean-ice GCM with prescribed climate change surface forcing, though the recovery in this case started after a few decades and full recovery took some thousands of years (Jansen et al., 2018). In another experiment in which the Central American seaway was artificially opened at Panama, the Atlantic freshening that occurred following exchange with the Pacific similarly induced an AMOC weakening and subsequent partial recovery starting after about 150 years (Brierley and Fedorov, 2016).
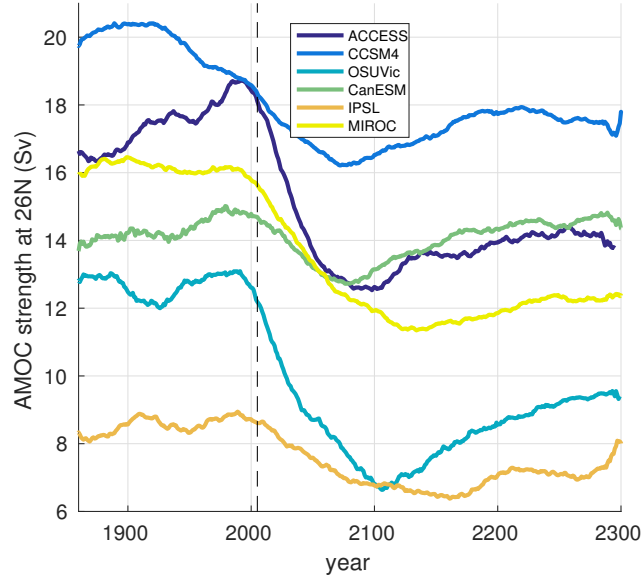
Figure 1. The AMOC strength at 26°N in all AMOCMIP ensemble members forced with the RCP4.5 emissions scenario Bakker et al. (2016). A 40 yr running mean has been applied. The dashed vertical line indicates the transition from historical forcing to RCP4.5 forcing. Units are Sv (1 Sv=10^6 m^3 s^{-1}).

Further support for a possible future AMOC recovery under sustained and modest climate change forcing can now also be found from the Coupled Model Intercomparison Project Phase 5 (CMIP5, Cheng et al., 2013) and the more recent AMOC Model Intercomparison Project (AMOCMIP, Bakker et al., 2016). Fig. 1 shows the AMOCMIP timeseries at 26°N for the historical and climate change scenarios of all long ensemble members forced with RCP4.5 forcing (Thomson et al., 2011) (see supplementary text). In each of these ensemble members the AMOC first weakens before beginning to recover after ∼100 years. This may demonstrate that such an AMOC recovery is a possibly robust feature among climate models. It should be noted, however, that the model run times were too short to establish whether the recovery would persist.

In this paper we demonstrate that the AMOC, when exposed to a sustained climate change freshwater flux (FWF) at high northern latitudes, can partially recover if the forcing does not exceed a critical threshold that would cause an AMOC collapse. We identify and isolate the mechanisms of this partial recovery in controlled freshwater experiments with a fully coupled configuration of the Community Earth System Model (CESM, Danabasoglu et al., 2012). To then test the hypotheses that the recovery can be brought

about by an oceanic-only mechanism controlled by 2D dynamics in the North Atlantic, we also use a 2D zonally-averaged Atlantic ocean-only model (Sevellec and Fedorov, 2011). We then demonstrate further how the occurrence of subsurface warming of the ocean implies an even more pronounced recovery of the MHT (Sevellec and Fedorov, 2016).

2 Numerical Models and Experiments

We performed freshwater hosing experiments with a fully coupled model and an idealized ocean-only model, in which a modest freshwater flux that is sustained in time and does not collapse the AMOC is designed to mimic a future melting of Greenland. However, the experiments can also be considered applicable to paleo considerations of glacial melt (e.g. of the Laurentide ice sheet), or as idealized representations of changes to the hydrological cycle or surface warming.

The coupled model we use is the Community Earth System Model (CESM, version 1, (Danabasoglu et al., 2012)), configured according to the gx1v6 global configuration with pre-industrial CO_2 levels that employs ocean, atmosphere, sea ice and land models. The POP2 ocean model has 60 staggered vertical levels, a zonal resolution of $1°$ and meridional resolution of $0.5°$ that decreases to $0.3°$ near the equator. The CAM5 atmosphere model has nominal $2°$ horizontal resolution. More information can be found at `http://www.cesm.ucar.edu/models/scientifically-supported.html`. The model pre-industrial control simulation has been spun-up from initial conditions for 900 years, at which point the simulation is extended for a further 250 years (presented as the model control run). Over this period the time-mean AMOC strength is ∼18 Sv at 26°N (1 Sv=10^6 $m^3 s^{-1}$), similar to the observations taken with the RAPID array (McCarthy et al., 2012). At year 900 (considered henceforth as year 0) two freshwater experiments were performed, in which a total FWF of magnitude of 0.1 Sv and 0.15 Sv was added uniformly into the surface layer of the grid cells immediately surrounding the lower half of Greenland (Fig. S1a). These fluxes were then maintained for 630 years. We conserve freshwater in the model by balancing the positive flux by an evenly distributed removal of freshwater from the rest of the global ocean surface, done so as to both better compare to the 2D model (described below) and also to allow the FWF to represent a change in the hydrological cycle (Held and Soden, 2006).
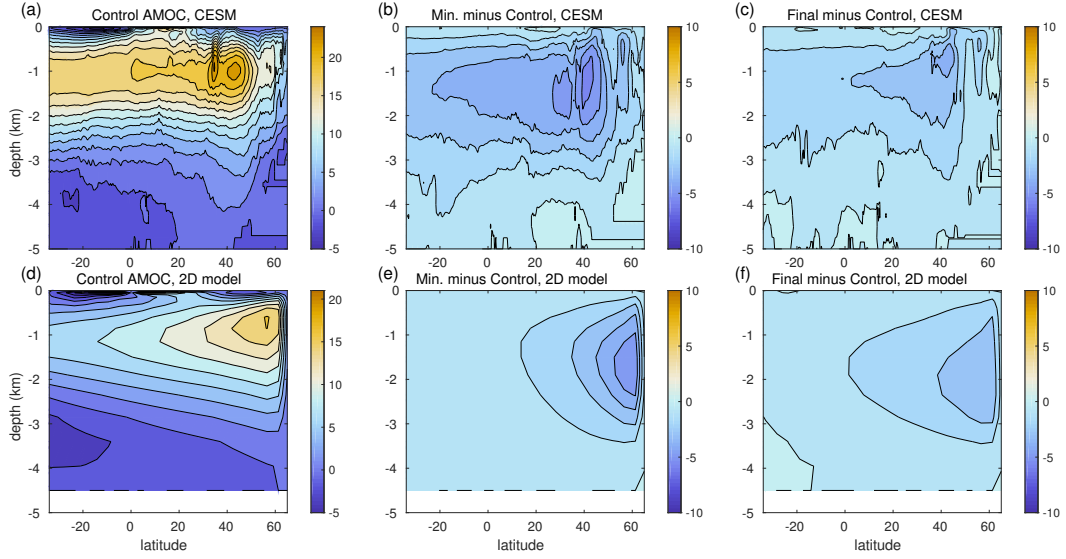
Figure 2. AMOC Eulerian streamfunctions for (a-c) CESM and (d-f) the 2D model. (a,d) Time mean streamfunction in the control experiment, and its change in perturbation experiments relative to the control (b,e) when the AMOC strength is minimum and (c,f) when the AMOC reaches a quasi-equilibrium (years 400-420). The CESM and 2D-model experiments use 0.1 Sv and 25 cm yr^{-1} of freshwater forcing, respectively. Units are Sv.

The imposed freshwater fluxes can be compared to an estimate that Greenland meltwater will reach ∼0.067 Sv by 2100 if rates of melting continue at the same observed acceleration (Swingedouw et al., 2013). However, while changes in freshwater forcing cannot be considered to induce the same response as a change in surface warming, our experiments are intended to provide an idealized representation of the combined effect of future forcing from meltwater, and changes in hydrological cycle and heat fluxes.

We also use an idealized zonally averaged ocean-only model of the Atlantic and Southern Oceans (Sevellec and Fedorov, 2011). The model has prognostic equations for temperature and salinity, which each include terms (with adjustable coefficients) for advection, isopycnal and diapycnal diffusion, convection and surface forcing. Idealized forcing terms take the form of mixed surface boundary conditions: surface temperature restoring (Fig. S2a), and fixed surface salinity flux (Fig. S2b) and wind stress (Fig. S2c). Convection occurs as an instantaneous adjustment to an unstable water column. Density is calculated according to a linear equation of state, and the pressure field is hydrostatic. Meridional velocities are diagnosed according to the meridional pressure gradient scaled

by a linear friction coefficient, as well as Ekman transport and eddy-induced velocities (Gent and McWilliams, 1990). The model latitude range is 66°S to 66°N with a horizontal resolution of ∼4.5° and 15 staggered vertical levels. Coefficients for horizontal and vertical diffusivity are 10^3 and 10^{-4} m^2 s^{-1} respectively, unless stated otherwise. Assuming the Atlantic basin width of 5100 km, transport fluxes can be calculated in units of Sv. (See Sevellec and Fedorov, 2011, for a full description of the model terms, parameters and forcing profiles, as well as discussion of assumptions such as scaling the AMOC with meridional pressure gradients). Note that while surface temperature restoring provides a negative feedback that helps maintain model stability, it may also constrain how the temperature can respond to freshwater forcing. The conclusions, however, are not sensitive to a doubling or halving of the default temperature restoring timescale of 1/66 days^{-1}.

The 2D model serves a number of valuable purposes in this study: 1) it allows us to verify that the recovery mechanism is an ocean-only mechanism that is not related to atmospheric feedbacks, and confined to the North Atlantic; 2) it can be used to verify that the AMOC and MHT responses to a high latitude FWF are driven by two dimensional dynamics on a depth-latitude plane; 3) it allows us to more easily explore the sensitivity of the AMOC response to different model parameters and freshwater fluxes, which is not possible with the expensive CESM configuration; 4) the model is simple enough to explore the above points while retaining important dynamics such as convection.

We employ the well tested 2D model control parameters reported by Sevellec and Fedorov (2011), in which the basin-wide maximum AMOC strength (see SI text) is realistic (Fig. 2c). Hosing experiments have then been performed for 5000 years, using a Gaussian latitude-profile FWF centred at 60°N and spanning the subpolar gyre (Fig. S1b). Freshwater is conserved throughout the duration of the runs by balancing the positive influx at the surface of the rest of the model, a necessary step in order to produce realistic results. Experiments using peak freshwater fluxes of 25 cm yr^{-1} and 35 cm yr^{-1} (equivalent to ∼0.08 Sv and ∼0.11 Sv respectively when integrated over the anomaly profiles) have been applied since their results resemble the coupled model freshwater experiments. Sensitivity experiments to FWF have then included a range of fluxes between 10 cm yr^{-1} and 90 cm yr^{-1} (∼0.03 Sv and ∼0.28 Sv respectively). Further sensitivity tests to FWF were also conducted with different values of vertical diffusivity and Southern Ocean wind stress, as reported later.
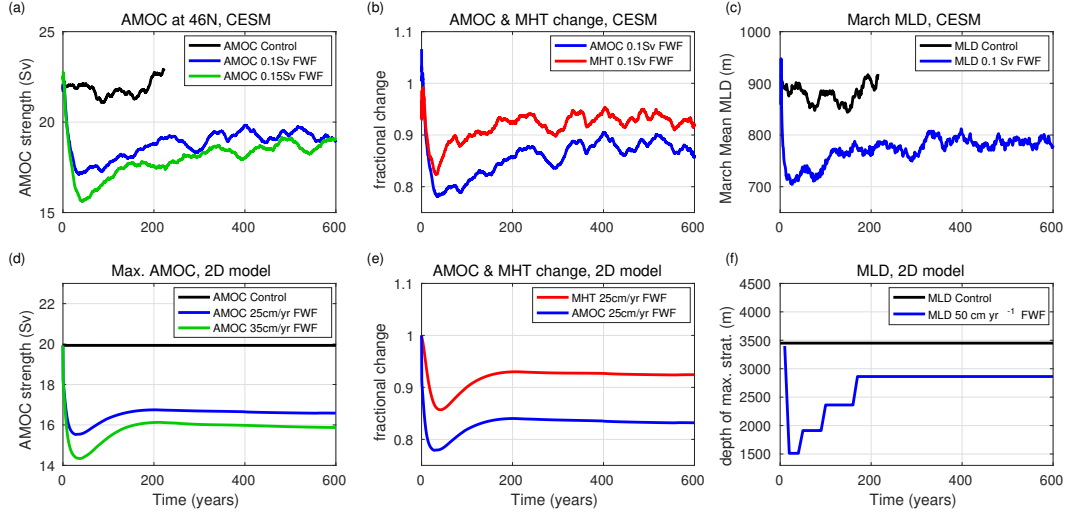
Figure 3. (a-c) CESM and (d-f) 2D model time series for several freshwater forcings: (a,d) the maximum control and freshwater AMOC strengths, (b,e) the normalized AMOC and MHT strengths of the 0.1 Sv FWF CESM and 25 cm yr^{-1} 2D model experiments, calculated relative to the time-mean control strengths (21.9 Sv and 0.63 PW for CESM respectively, and 19.9 Sv and 0.62 PW for the 2D model respectively), and (c,f) the average mixed layer depth within the convection regions. A 40-year smoothing was applied. The AMOC strength includes parameterized eddy contributions. Mixed layers are calculated as the March-mean depth within convection regions (CESM) and as the depth of maximum density stratification in the downwelling region (2D model).

3 Results

We first demonstrate how the AMOC responds in the model FWF experiments in both the fully coupled configuration of CESM and in the 2D model (see methods). We then discuss the ocean property changes and mechanisms that are responsible for the AMOC recovery and the stronger re-invigoration of the MHT (see SI text for calculations of the AMOC, MHT and mixed layer depth; Marshall et al., 1993; Schmidtko et al., 2013; Thomas and Fedorov, 2017).

3.1 AMOC response to a moderate FWF

Fig. 3a shows the AMOC timeseries of the control and the two FWF experiments at 46°N in the CESM configuration, 40-yr smoothed to highlight the multidecadal changes. As expected from previous studies using similar magnitude freshwater fluxes (Barreiro

et al., 2008; Smith et al., 2014; Swingedouw et al., 2013), the model AMOC in the experiments initially weakens in response to the increase in high latitude stratification, decreasing in the 0.1 Sv FWF run from ∼22 Sv to ∼17 Sv over the first ∼40 years at a rate of ∼0.12 Sv yr^{-1}. For context, this rate is close to an observed estimate of 0.13 Sv yr^{-1} derived from satellite and cable data at 26°N between 1993-2014, although this trend was found to not be significant and might reflect natural ocean variability (Frajka-Williams, 2015).

After 40 years the model AMOC starts to recover, which supports our hypothesis and, as discussed below, is consistent with a gradual subsurface erosion of the high latitude stratification that partly re-invigorates deep convection. Recovery continues for the next 350 years, strengthening by a total of ∼2.2 Sv until a new near-steady state is reached. To test the sensitivity of the AMOC recovery to the strength of the FWF, the experiment has been repeated using a FWF of 0.15 Sv. This flux induces the same pattern of weakening and recovery, reaching a ∼1 Sv weaker AMOC strength than in the 0.1 Sv FWF experiment (Fig. 3a).

To test sensitivity to the initial conditions, the 0.1 Sv FWF experiment was also repeated starting at an earlier period of the control simulation, and the results were closely reproduced (Fig. S3). This experiment was run for 950 years to verify that the AMOC reached a new near-equilibrium state. It is noteworthy that in numerical experiments using weakly-enhanced surface warming (Jansen et al., 2018) and CO_2 forcing (Manabe and Stouffer, 1994) the simulated AMOC can make an eventual full recovery. Consistent with Jansen et al. (2018), we suggest that our North Atlantic mechanism controls an initial centennial timescale AMOC adjustment, while longer timescale changes are brought about by Southern Ocean adjustments that are excluded from our experimental design.

We now use the 2D model FWF experiments to test whether both the initial weakening and eventual recovery can be largely explained according to two dimensional ocean-only dynamics. The AMOC response in the simpler model is qualitatively very similar to that of the coupled model (Fig. 3a,d), with a timescale before recovery of about 35 years and an eventual 1.5 Sv recovery from a minimum value of 15.5 Sv in the 25 cm yr^{-1} experiment. Despite a faster recovery timescale in the 2D model, the agreement is striking given the large differences between the two models. Changes in the streamfunction

214 in both models, displayed for both the minimum value (years 35-55 average; Fig. 2b,e)

215 and its near-equilibrium state (years 400-420 average; Fig. 2c,f), reveal reductions in AMOC

216 strength that are similarly produced in both models. The high northern latitude-centered

217 AMOC changes are consistent with a buoyancy-driven AMOC change (Eden and Wille-

218 brand, 2001).

219   To test that the AMOC response to increased FWF is a consistent response across

220 parameter space in the 2D model, we have modified the magnitude of the FWF, the sur-

221 face temperature restoring timescale, the horizontal diffusivity, vertical diffusivity (Fig.

222 S4), and the wind stress over the Southern Ocean (Fig. S4). See Fig. S1c and Fig. S2c

223 for the surface wind stress profiles, and Sevellec and Fedorov (2011) for its application

224 in the model equations. We find that the occurrence of an AMOC recovery is robust across

225 a broad range of parameters (that provide reasonable temperature, salinity and density

226 fields and retain an active AMOC). However, the time when recovery begins (ranging

227 from ~30-300 years), the minimum AMOC strength before recovery (down to ~8 Sv),

228 the timescale to equilibrium, and the recovery magnitude do depend on the parameters,

229 indicating that model dependency is a factor. Of these, the first two are most sensitive

230 to the magnitude of the FWF; discussed below), and the latter two are most strongly

231 affected by the magnitudes of the vertical diffusivity and Southern Ocean wind stress

232 (Fig. S4): increased vertical diffusivity leads to a longer equilibrium timescale and a weaker

233 recovery relative to the peak minimum, and vice versa for the wind stress (see section

234 3.2 for a hypothesis to explain this result). Such model sensitivities may explain the dif-

235 ferent responses to forcing changes exhibited between the AMOCMIP model members

236 (Fig. 1 Bakker et al., 2016) and their differences to the faster recovery time in our CESM

237 configuration (see Swingedouw et al., 2013, for an evaluation of model dependent responses

238 to 0.1 Sv hosing).

239   Fig. S4 shows the 2D model sensitivity to increasing values of freshwater in each

240 of the 2D model parameter-sensitivity experiments. We focus on the experiment with

241 default parameter settings shown in the middle subpanel (Fig. S4e). While the shape

242 of the decline and recovery is similar across all forcing strengths at or below 70 cm yr^{-1},

243 the timescale to the AMOC minimum increases with freshwater forcing. This is likely

244 because larger subsurface changes must first develop to overcome a larger stratification.

245 The AMOC state has a sudden bifurcation point, collapsing at ~70.1 cm yr^{-1}. At the

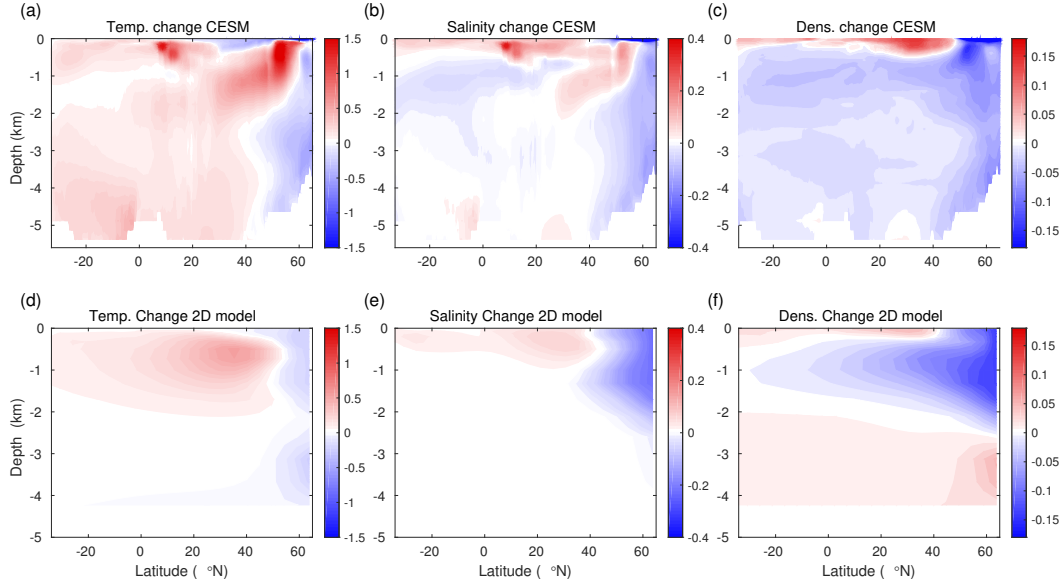246 freshwater forcing value of 70 cm yr^{-1} the AMOC takes ~200 years before a recovery

Figure 4. The Atlantic-zonally averaged (a-c) 0.1 Sv CESM and (d-f) 25 cm yr^{-1} 2D model changes in (a,d) temperature ($^{\circ}$C), (b,e) salinity and (c,f) density (kg m^{-3}), calculated at the time of minimum AMOC strength (years 30-50 average) relative to the time-mean control values (minimum minus control).

occurs. We note that this strong sensitivity to the freshwater forcing happens only in a narrow range of freshwater fluxes just before the bifurcation point. At a stronger forcing than 70.1 cm yr^{-1} the AMOC collapses increasingly rapidly. Similar behavior in response to stronger FWF forcing also occurs when employing different model parameter values for vertical diffusivity or Southern Ocean wind stress, though each has a different FWF value at the bifurcation (Fig. S4).

3.2 Mechanisms of AMOC recovery and impact on MHT

To elucidate the mechanisms of the AMOC recovery in the two models we show changes in the zonal-mean temperature, salinity and density fields at the time of minimum AMOC (Fig. 4), as well as their evolution over the first 90 years following increased freshwater forcing (Fig. S5, Fig. S6). We then compare these to the model high latitude March-mean Mixed Layer Depth (MLD) changes in the deep-convection regions (see SI text), which has previously been shown to be a good indicator of convective mixing and deep water formation on decadal to multi-decadal timescales (e.g. Eden and Willebrand, 2001; Spall and Pickart, 2001; Thomas et al., 2015). The initial freshening is confined

to the upper ocean at high latitude (Fig. S5, Fig. S6) and induces a rapid weakening in convection, as indicated by a shoaling of the high latitude MLD (Fig. 3c,f), and a weakening of the AMOC (Fig. 3a,d). Similar to previous findings (Barreiro et al., 2008; Fedorov et al., 2007; Liu et al., 2009; Marcott et al., 2011; Mignot et al., 2007; Sevellec and Fedorov, 2015), this is accompanied at first by high latitude surface cooling due to a weakened northwards MHT, and subsurface warming possibly due to weaker convection (Fig. S5, Fig. S6). Initially small in magnitude, subsurface temperature anomalies in both models then grow and move southwards, being replaced over the first decade by a high latitude cooling signature at all depths (Fig. 4a,d, Fig. S5, Fig. S6). Along with downwards diffusion of the surface signature, the development of the high latitude cooling is largely a consequence of the still-active AMOC that advects and mixes the surface signal downwards (Fig. S7). Subsurface freshening similarly takes place at high latitudes (Fig. 4b,e, Fig. S5, Fig. S6), countering the subsurface cooling and dominating density changes (Fig. 4c,f). The subsurface subtropical gyre then continues to warm, either because of weaker northwards heat transport along the subsurface pathway out of the subtropics (Mignot et al., 2007), leading to heat convergence, or because of weakened subtropical upwelling under a weaker AMOC (Manabe and Stouffer, 1994). The result of the property changes in both models is the development of a subsurface tongue of low density water at all latitudes that is controlled by both freshening at high latitudes and warming at low latitudes. After ∼40 years into the simulations, changes in the high latitude vertical density gradient bring about an AMOC recovery as the signature propagates southwards.

This recovery mechanism, brought about by reduction in subsurface density, may help explain the AMOC response to increased Southern Ocean wind stress and increased diffusivity, which respectively enhance and suppress the recovery magnitude and timescales (as mentioned in the previous subsection; Fig. S4). While increases in both parameters act to strengthen the AMOC, which might be expected to enhance the recovery through more rapid development of the subsurface signature, a higher diffusivity may hinder its development by diffusing away the signal. Further work is needed however to test this hypothesis.

Of greater importance for the climate is the response of the MHT to the freshwater flux. Subtropical warming, while strongest in the subsurface, occurs within the northwards branch of the AMOC in both models. Therefore, although the AMOC weakens following increased freshwater input, it becomes more efficient by transporting warmer

295   water (Sevellec and Fedorov, 2016). Accordingly, in the two models we find that the rel-

296   ative weakening of the MHT is less pronounced than that of the AMOC volume trans-

297   port, when calculated relative to their control mean strengths (Fig. 3b,d). This is the

298   case at all latitudes where warming occurs, including northwards and southwards of the

299   subtropics, and is therefore not related to the transport of heat by the gyre. This is fur-

300   ther evidenced by the similar MHT response in the 2D model, in which there is only an

301   AMOC change.

4 Conclusions

303   Using freshwater experiments applied to a fully coupled model and a zonally-averaged

304   ocean model, in which freshwater was artificially fluxed into the surface of the high lat-

305   itude North Atlantic, we have demonstrated that the AMOC, and particularly its asso-

306   ciated heat transport, can partially recover under sustained high latitude climate change

307   forcing. A similarity in the responses of the two models to freshwater forcing demonstrates

308   that the recovery is an oceanic-only mechanism that emerges in a 2D framework. How-

309   ever, it requires that the ocean retains an active AMOC, necessitating that greenhouse

310   gas emissions do not exceed a threshold magnitude. In climate models (Bakker et al.,

311   2016; Cheng et al., 2013) this critical threshold is exceeded in all projections with the

312   RCP8.5 emissions.

313   In our freshwater forcing experiments the onset of a recovery is due to a negative

314   climate feedback that can initiate the recovery after some 40 years of initial weakening.

315   The mechanism is brought about by gradual high latitude subsurface freshening, caused

316   by the downwards advection and convection of freshwater by the still-active AMOC (Fig.

317   4b,e). This erodes the initial stratification imposed by surface freshening, thus re-invigorating

318   convection (Fig. 3c,f) and the AMOC (Fig. 3a,d). Subsequent subsurface subtropical

319   warming (Fig. 4a,d) then ensures that the MHT weakens less than the AMOC volume

320   transport (Fig. 3b,e). Although the magnitudes of the initial weakening, the subsequent

321   recovery, and the timescale to recovery are all sensitive to the choices of the 2D model

322   parameters, the occurrence of a recovery is a robust feature across parameter space (Fig.

323   S4). The mechanism of recovery in our experiments, through the downwards transfer of

324   high latitude surface freshwater, is different to our initial hypothesis that subsurface warm-

325   ing re-invigorates convection. Further work is needed to assess whether future surface

326   heating applied to the subolar North Atlantic would yield similar results following the

downwards transfer of warm surface temperatures, such as may be occurring in AMOCMIP (Bakker et al., 2016).

In CESM, forced with a 0.1 Sv FWF that is artificially injected around southern Greenland, a minimum AMOC weakening that peaks at a 22% reduction eventually comes into an equilibrium state in which the MHT is weakened by only 7%. One possible implication of this recovery can be seen in the relative changes in sea surface temperature (SST) between the AMOC minimum and its final equilibrated state (Fig. S8). In the 0.1 Sv FWF CESM experiment, large SST increases of up to 2°C occur in the North Atlantic and Nordic Seas following the recovery, however it is not clear to what extent this is related to coupled atmosphere-ocean feedbacks (e.g. Zhang et al., 2010) and requires future research. Our results also challenge the commonly held perception of a one-to-one relationship between the AMOC and the MHT, which does not account for possible relative changes in the vertical profiles of temperature and velocity. Finally, the model temperature and salinity changes that prime the AMOC recovery resemble those observed to have taken place in the Atlantic ocean with depth during the second half of the 20th century (Curry et al., 2003; Levitus et al., 2000). Future work will be required to assess if these changes are due to the mechanisms we describe here, and whether they could bring about a partial recovery during a potential AMOC decline (Caesar et al., 2018; Thornalley et al., 2018).

References

P. Bakker, A. Schmittner, J. T. M. Lenaerts, A. Abe-Ouchi, D. Bi, M. R. van den Broeke, W. L. Chan, A. Hu, R. L. Beadling, S. J. Marsland, S. H. Mernild, O. A. Saenko, D. Swingedouw, A. Sullivan, and J. Yin.   Fate of the Atlantic Meridional Overturning Circulation: Strong decline under continued warming and Greenland melting. *Geophysical Research Letters*, 43(23):12252–12260, December 2016. 10.1002/2016GL070457.

M. Barreiro, A. Fedorov, R. Pacanowski, and S. G. Philander.   Abrupt climate changes: How freshening of the northern Atlantic affects the thermohaline and wind-driven oceanic circulations. *Annual Review of Earth and Planetary Sciences*, 36:33–58, 2008. 10.1146/annurev.earth.36.090507.143219.

C. M. Brierley and A. V. Fedorov.   Comparing the impacts of Miocene-Pliocene changes in inter-ocean gateways on climate: Central American seaway, Bering strait, and Indonesia. *Earth and Planetary Science Letters*, 444:116–130, June 2016. 10.1016/j.epsl.2016.03.010.

S. E. Brunnabend and H. A. Dijkstra.   Asymmetric response of the Atlantic Meridional Ocean Circulation to freshwater anomalies in a strongly-eddying global ocean model.   *Tellus Series A-dynamic Meteorology and Oceanography*, 69: 1299283, 2017. 10.1080/16000870.2017.1299283.

L. Caesar, S. Rahmstorf, A. Robinson, G. Feulner, and V. Saba.   Observed fingerprint of a weakening Atlantic Ocean overturning circulation.   *Nature*, 556 (7700):191–+, April 2018. 10.1038/s41586-018-0006-5.

L. J. Cheng, K. E. Trenberth, J. Fasullo, T. Boyer, J. Abraham, and J. Zhu.   Improved estimates of ocean heat content from 1960 to 2015. *Science Advances*, 3 (3):e1601545, March 2017. 10.1126/sciadv.1601545.

W. Cheng, J. C. H. Chiang, and D. X. Zhang. Atlantic Meridional Overturning Circulation (AMOC) in CMIP5 models: RCP and Historical simulations. *Journal of Climate*, 26(18):7187–7197, September 2013. 10.1175/JCLI-D-12-00496.1.

R. Curry, B. Dickson, and I. Yashayaev.   A change in the freshwater balance of the Atlantic Ocean over the past four decades. *Nature*, 426(6968):826–829, December 2003. 10.1038/nature02206.

G. Danabasoglu, S. C. Bates, B. P. Briegleb, S. R. Jayne, M. Jochum, W. G. Large, S. Peacock, and S. G. Yeager.   The CCSM4 ocean component.   *Journal of*

Climate, 25(5):1361–1389, March 2012. 10.1175/JCLI-D-11-00091.1.

M. den Toom, H. A. Dijkstra, W. Weijer, M. W. Hecht, M. E. Maltrud, and E. van Sebille. Response of a strongly eddying global ocean to North Atlantic freshwater perturbations. *Journal of Physical Oceanography*, 44(2):464–481, February 2014. 10.1175/JPO-D-12-0155.1.

C Eden and J Willebrand. Mechanism of interannual to decadal variability of the North Atlantic circulation. *J. Climate*, 14(10):2266–2280, 2001.

A. Fedorov, M. Barreiro, G. Boccaletti, R. Pacanowski, and S. G. Philander. The freshening of surface waters in high latitudes: Effects on the thermohaline and wind-driven circulations. *Journal of Physical Oceanography*, 37(4):896–907, April 2007. 10.1175/JPO3033.1.

E. Frajka-Williams. Estimating the Atlantic overturning at 26 degrees N using satellite altimetry and cable measurements. *Geophysical Research Letters*, 42(9): 3458–3464, May 2015. 10.1002/2015GL063220.

P R Gent and J C Mcwilliams. Isopycnal Mixing In Ocean Circulation Models. *J. Phys. Oceanogr.*, 20(1):150–155, jan 1990. 10.1175/1520-0485(1990)020⟨0150: IMIOCM⟩2.0.CO;2.

I. M. Held and B. J. Soden. Robust responses of the hydrological cycle to global warming. *Journal of Climate*, 19(21):5686–5699, November 2006. 10.1175/JCLI3990.1.

IPCC. *Climate Change 2013: The Physical Science Basis. Contribution of Working Group I to the Fifth Assessment Report of the Intergovernmental Panel on Climate Change.* Cambridge University Press, Cambridge, United Kingdom and New York, NY, USA, 2013. ISBN ISBN 978-1-107-66182-0. 10.1017/CBO9781107415324. URL www.climatechange2013.org.

L Jackson and M Vellinga. Multidecadal to Centennial Variability of the AMOC:HadCM3 and a purturbed Physics Ensemble. *J. Climate*, 26:2390–2407, 2013.

M Jansen, L-P Nadeau, and T M Merlis. Transient versus equilibrium response of the oceans overturning circulation to warming. *J. Climate*, 31:5147–5163, 2018.

T Kanzow, S A Cunningham, D Rayner, J J M Hirschi, W E Johns, M O Baringer, H L Bryden, L M Beal, C S Meinen, and J Marotzke. Observed flow compensation associated with the MOC at 26.5 degrees N in the Atlantic. *Science*, 317

(5840):938–941, 2007.

S Levitus, J I Antonov, T P Boyer, and C Stephens. Warming of the world ocean. *Science*, 287(5461):2225–2229, 2000.

W. Liu, S. P. Xie, Z. Y. Liu, and J. Zhu. Overlooked possibility of a collapsed Atlantic Meridional Overturning Circulation in warming climate. *Science Advances*, 3(1):e1601666, January 2017. 10.1126/sciadv.1601666.

Z. Liu, B. L. Otto-Bliesner, F. He, E. C. Brady, R. Tomas, P. U. Clark, A. E. Carlson, J. Lynch-Stieglitz, W. Curry, E. Brook, D. Erickson, R. Jacob, J. Kutzbach, and J. Cheng. Transient simulation of last deglaciation with a new mechanism for Bolling-Allerod warming. *Science*, 325(5938):310–314, July 2009. 10.1126/science.1171041.

M. S. Lozier, S. Bacon, A. S. Bower, S. A. Cunningham, M. F. de Jong, L. de Steur, B. deYoung, J. Fischer, S. F. Gary, B. J. W. Greenan, P. Heimbach, N. P. Holliday, L. Houpert, M. E. Inall, W. E. Johns, H. L. Johnson, J. Karstensen, F. L. Li, X. P. Lin, N. Mackay, D. P. Marshall, H. Mercier, P. G. Myers, R. S. Pickart, H. R. Pillar, F. Straneo, V. Thierry, R. A. Weller, R. G. Williams, C. Wilson, J. Y. Yang, J. Zhao, and J. D. Zika. Overturning in the subpolar North Atlantic program a new international ocean observing system. *Bulletin of the American Meteorological Society*, 98(4):737–752, April 2017. 10.1175/BAMS-D-16-0057.1.

S. Manabe and R. J. Stouffer. Multiple-century response of a coupled ocean-atmosphere model to an increase of atmospheric carbon-dioxide. *Journal of Climate*, 7(1):5–23, January 1994. 10.1175/1520-0442(1994)007⟨0005: MCROAC⟩2.0.CO;2.

S. A. Marcott, P. U. Clark, L. Padman, G. P. Klinkhammer, S. R. Springer, Z. Y. Liu, B. L. Otto-Bliesner, A. E. Carlson, A. Ungerer, J. Padman, F. He, J. Cheng, and A. Schmittner. Ice-shelf collapse from subsurface warming as a trigger for Heinrich events. *Proceedings of the National Academy of Sciences of the United States of America*, 108(33):13415–13419, August 2011. 10.1073/pnas.1104772108.

J C Marshall, A J G Nurser, and R G Williams. Inferring the subduction rate and period over the North-Atlantic. *J. Phys. Oceanogr.*, 23(7):1315–1329, jul 1993. 10.1175/1520-0485(1993)023⟨1315:ITSRAP⟩2.0.CO;2.

G McCarthy, E Frajka-Williams, W E Johns, M O Baringer, C S Meinen, H L Bryden, D Rayner, A Duchez, C Roberts, and S A Cunningham. Observed interannual variability of the Atlantic Meridional Overturning Circulation at 26.5 degrees N. *Geophys. Res. Lett.*, 39:L19609, oct 2012.

L. Menviel, A. Timmermann, T. Friedrich, and M. H. England. Hindcasting the continuum of dansgaard-oeschger variability: mechanisms, patterns and timing. *Climate of the Past*, 10(1):63–77, 2014. 10.5194/cp-10-63-2014.

J. Mignot, A. Ganopolski, and A. Levermann. Atlantic subsurface temperatures: Response to a shutdown of the overturning circulation and consequences for its recovery. *Journal of Climate*, 20(19):4884–4898, October 2007. 10.1175/JCLI4280.1.

S. Rahmstorf. Ocean circulation and climate during the past 120,000 years. *Nature*, 419(6903):207–214, September 2002. 10.1038/nature01090.

S. Rahmstorf, J. E. Box, G. Feulner, M. E. Mann, A. Robinson, S. Rutherford, and E. J. Schaffernicht. Exceptional twentieth-century slowdown in Atlantic Ocean overturning circulation. *Nature Climate Change*, 5(5):475–480, May 2015. 10.1038/NCLIMATE2554.

T. L. Rasmussen and E. Thomsen. The role of the North Atlantic drift in the millennial timescale glacial climate fluctuations. *Palaeogeography Palaeoclimatology Palaeoecology*, 210(1):101–116, July 2004. 10.1016/j.palaeo.2004.04.005.

P Rhines, S Häkkinen, and S A Josey. Is the oceanic heat transport significant in the climate system? In R R Dickson, J Meincke, and P Rhines, editors, *ArcticSubarctic Ocean Fluxes: Defining the Role of the Northern Seas in Climate*, pages 111–130. Springer, Dordrecht, Netherlands, 2008.

C. Ruhlemann, S. Mulitza, G. Lohmann, A. Paul, M. Prange, and G. Wefer. Intermediate depth warming in the tropical Atlantic related to weakened thermohaline circulation: Combining paleoclimate data and modeling results for the last deglaciation. *Paleoceanography*, 19(1):PA1025, March 2004. 10.1029/2003PA000948.

S. Schmidtko, G. C. Johnson, and J. M. Lyman. Mimoc: A global monthly isopycnal upper-ocean climatology with mixed layers. *Journal of Geophysical Research-oceans*, 118(4):1658–1672, April 2013. 10.1002/jgrc.20122.

F. Sevellec and A. V. Fedorov. Stability of the Atlantic Meridional Overturning Circulation and stratification in a zonally averaged ocean model: Effects of freshwater flux, southern ocean winds, and diapycnal diffusion. *Deep-sea Research Part Ii-topical Studies In Oceanography*, 58(17-18):1927–1943, September 2011. 10.1016/j.dsr2.2010.10.070.

F. Sevellec and A. V. Fedorov. AMOC sensitivity to surface buoyancy fluxes: Stronger ocean meridional heat transport with a weaker volume transport? *Climate Dynamics*, 47(5-6):1497–1513, September 2016. 10.1007/s00382-015-2915-4.

F. Sevellec and A. V. Fedorov. Optimal excitation of AMOC decadal variability: Links to the subpolar ocean. *Progress In Oceanography*, 132:287–304, March 2015. 10.1016/j.pocean.2014.02.006.

F. Sevellec, A. V. Fedorov, and W. Liu. Arctic sea-ice decline weakens the Atlantic Meridional Overturning Circulation. *Nature Climate Change*, 7(8):604–610, August 2017. 10.1038/NCLIMATE3353.

R. S. Smith, R. Sutton, and J. M. Gregory. The impact of salinity perturbations on the future uptake of heat by the Atlantic Ocean. *Geophysical Research Letters*, 41(24):9072–9079, December 2014. 10.1002/2014GL062169.

M A Spall and R S Pickart. Where does dense water sink? A subpolar gyre example. *J. Phys. Oceanogr.*, 31:810–826, 2001.

D. Swingedouw, C. B. Rodehacke, E. Behrens, M. Menary, S. M. Olsen, Y. Q. Gao, U. Mikolajewicz, J. Mignot, and A. Biastoch. Decadal fingerprints of freshwater discharge around Greenland in a multi-model ensemble. *Climate Dynamics*, 41(3-4):695–720, August 2013. 10.1007/s00382-012-1479-9.

M. D. Thomas and A. V. Fedorov. The eastern subtropical pacific origin of the equatorial cold bias in climate models: A Lagrangian perspective. *Journal of Climate*, 30(15):5885–5900, August 2017. 10.1175/JCLI-D-16-0819.1.

M D Thomas, A-M Treguier, B Blanke, J Deshayes, and A Voldoire. A Lagrangian method to isolate the impacts of mixed layer subduction on the meridional overturning circulation in a numerical model. *J. Climate*, 28(19):7503–7517, oct 2015. 10.1175/JCLI-D-14-00631.1.

A. M. Thomson, K. V. Calvin, S. J. Smith, G. P. Kyle, A. Volke, P. Patel, S. Delgado-Arias, B. Bond-Lamberty, M. A. Wise, L. E. Clarke, and J. A.

Edmonds. RCP4.5: a pathway for stabilization of radiative forcing by 2100. *Climatic Change*, 109(1-2):77–94, November 2011. 10.1007/s10584-011-0151-4.

D. J. R. Thornalley, D. W. Oppo, P. Ortega, J. I. Robson, C. M. Brierley, R. Davis, I. R. Hall, P. Moffa-Sanchez, N. L. Rose, P. T. Spooner, I. Yashayaev, and L. D. Keigwin. Anomalously weak Labrador Sea convection and Atlantic overturning during the past 150 years. *Nature*, 556(7700):227–+, April 2018. 10.1038/s41586-018-0007-4.

M. Vellinga and R. A. Wood. Impacts of thermohaline circulation shutdown in the twenty-first century. *Climatic Change*, 91(1-2):43–63, November 2008. 10.1007/s10584-006-9146-y.

R A Wood, M Vellinga, and R Thorpe. Global warming and thermohaline circulation stability. *Philos. T. R. Soc. A*, 361(1810):1961–1974, sep 2003.

R. Zhang and T. L. Delworth. Simulated tropical response to a substantial weakening of the Atlantic thermohaline circulation. *Journal of Climate*, 18(12):1853–1860, June 2005. 10.1175/JCLI3460.1.

R. Zhang, S. M. Kang, and I. M. Held. Sensitivity of climate change induced by the weakening of the Atlantic Meridional Overturning Circulation to cloud feedback. *Journal of Climate*, 23(2):378–389, January 2010. 10.1175/2009JCLI3118.1.

X. Zhang, G. Knorr, G. Lohmann, and S. Barker. Abrupt North Atlantic circulation changes in response to gradual CO2 forcing in a glacial climate state. *Nature Geoscience*, 10(7):518–+, July 2017. 10.1038/NGEO2974.